

## Supporting Information

### Spacer-engineering construction of continuous proton transport networks for cardo poly(biphenyl indole) high-temperature proton exchange membranes

Sifan Chen,<sup>a</sup> Zhuang Ma,<sup>a</sup> Jialin Zhang,<sup>c</sup> Jianchun Niu,<sup>a</sup> Shuomeng Zhang,<sup>a</sup> Qinghua Zhang,<sup>\*a</sup> Shiyuan Chen,<sup>b</sup> Shanfu Lu,<sup>\*c</sup> Miao Wang<sup>b</sup> and Qinggang He<sup>\*a</sup>

<sup>a</sup>College of Chemical and Biological Engineering, Zhejiang University, Hangzhou 310027, China.

<sup>b</sup>Zhejiang Province Key Laboratory of Quantum Technology and Device, Department of Physics, Zhejiang University, Hangzhou 310027, China.

<sup>c</sup>School of energy and power engineering, Beihang University, Beijing, 100191, China.

E-mail: qghe@zju.edu.cn (Q. He); lusf@buaa.edu.cn (S. Lu); qhzhang@zju.edu.cn (Q. Zhang)

## Supporting figures

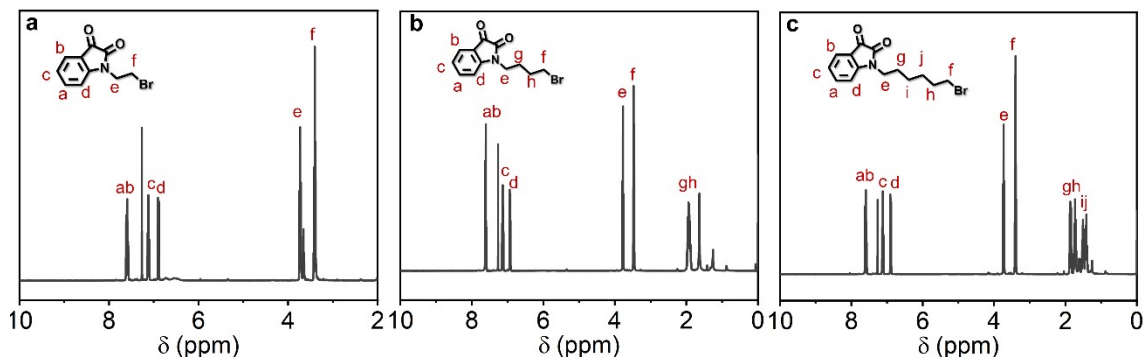


**Figure S1.** <sup>1</sup>H NMR spectrum of (a) OXIE, (b) OXIB and (c) OXIH in  $\text{CDCl}_3$ .

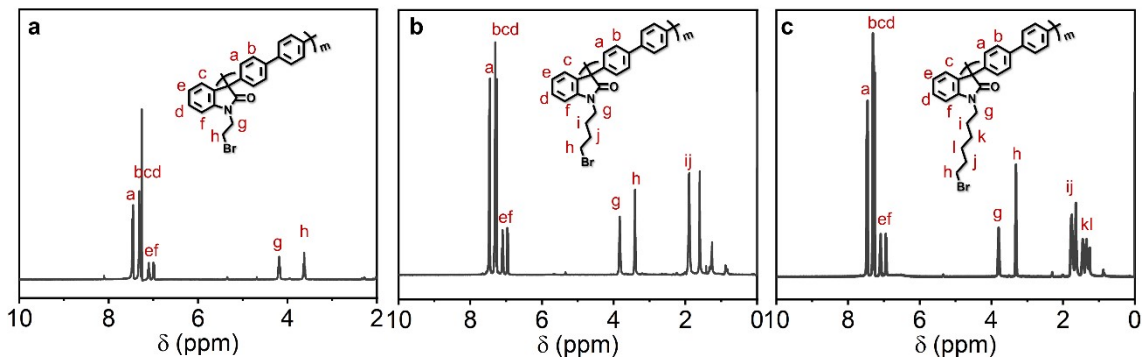


**Figure S2.** <sup>1</sup>H NMR spectrum of (a) POXIE, (b) POXIB and (c) POXIH in CDCl<sub>3</sub>. The <sup>1</sup>H NMR spectrum of POXIA show two new signals of 7-8 ppm (a and b) assigned to biphenyl protons, and the rest of the peak assignments were the same as those of OXIA.

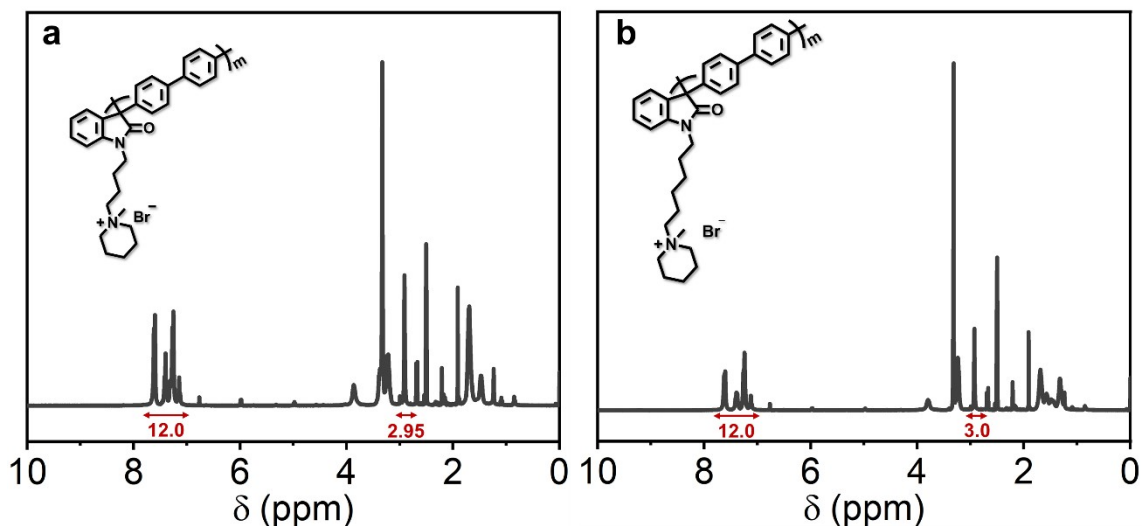


**Figure S3.** <sup>1</sup>H NMR spectrum of (a) POXIB and (b) POXIH in DMSO-*d*6. The two peaks at 2.92 ppm and 3.22 ppm are attributed to -CH<sub>3</sub> and -CH<sub>2</sub>- directly attached to the N atoms in QA. The quaternization efficiency can be calculated from the integral ratio of 2.92 ppm QA methyl protons to 7-8 ppm aromatic protons, which proves that the quaternization reaction is close to completion. The efficiency of quaternization could be calculated from the integral ratio of the aromatic proton (12 H) peaks at 7-8 ppm with the QA methyl protons (3 H) at 2.9 ppm.

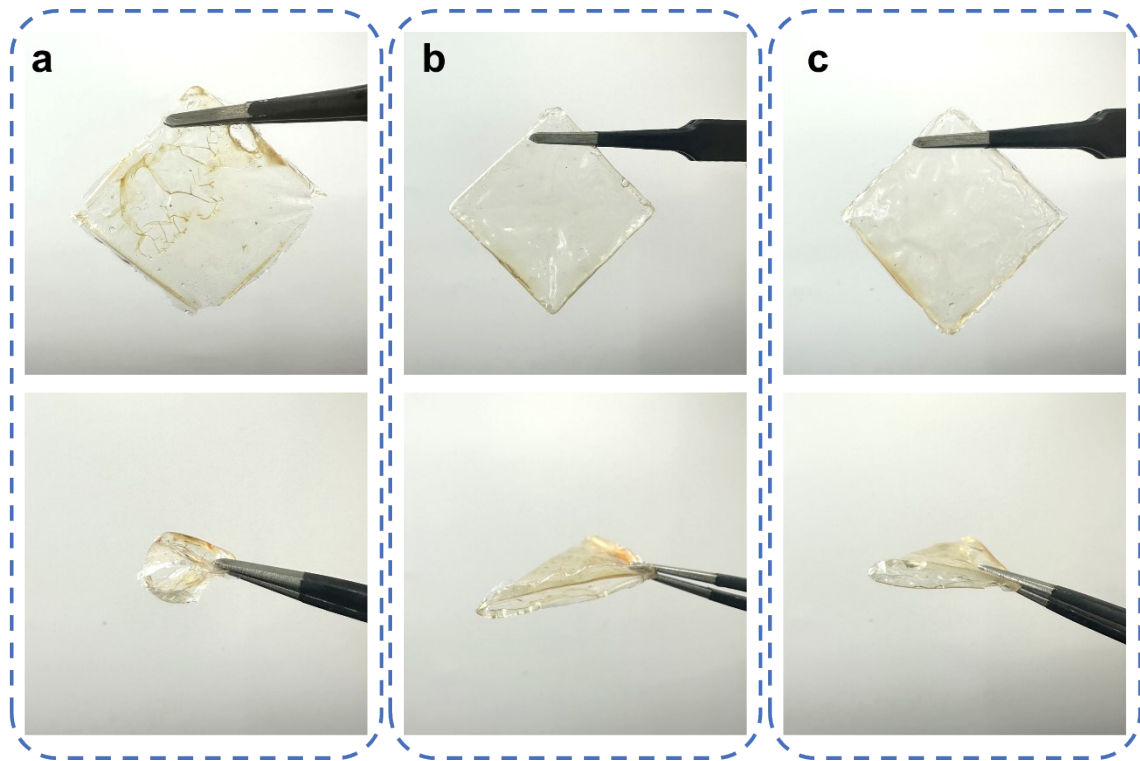


**Figure S4.** Digital photographs of (a) POXIE-QA, (b) POXIB-QA, (c) POXIH-QA.

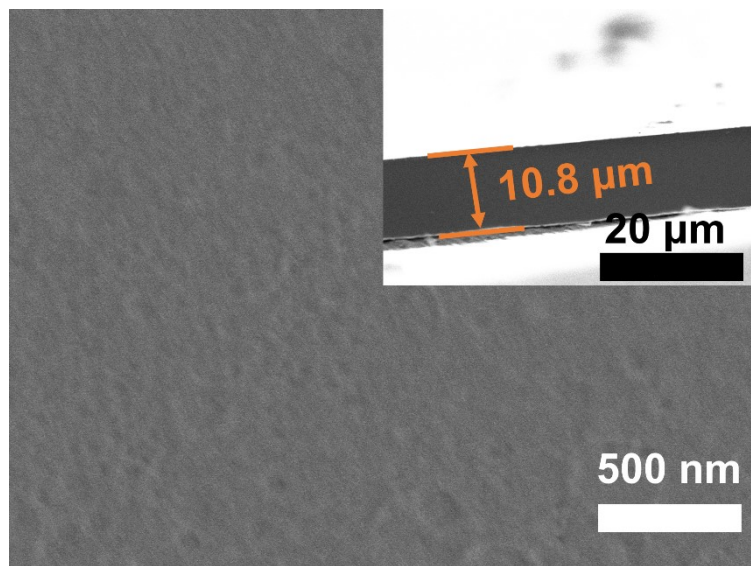


**Figure S5.** Top-view SEM image of POXIB-QA membrane. Inserted are the cross-section of the SEM image and the thickness of the membrane.

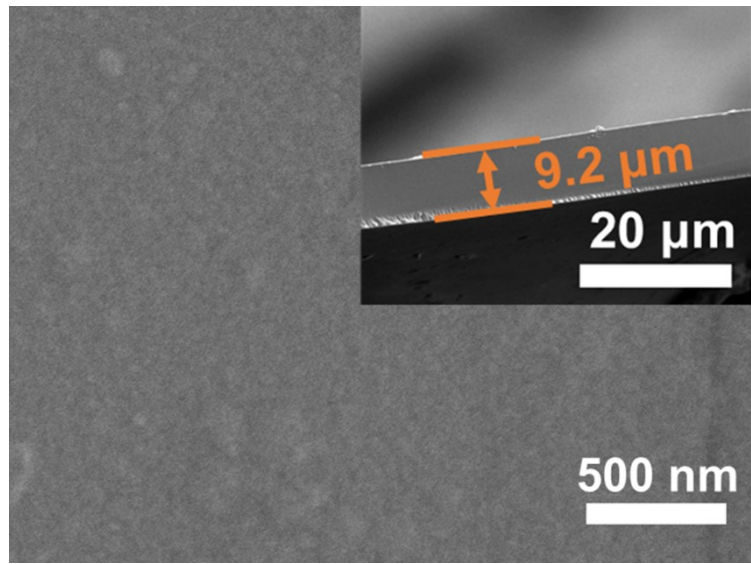


**Figure S6.** Top-view SEM image of POXIH-QA membrane. Inserted are the cross-section of the SEM image and the thickness of the membrane.

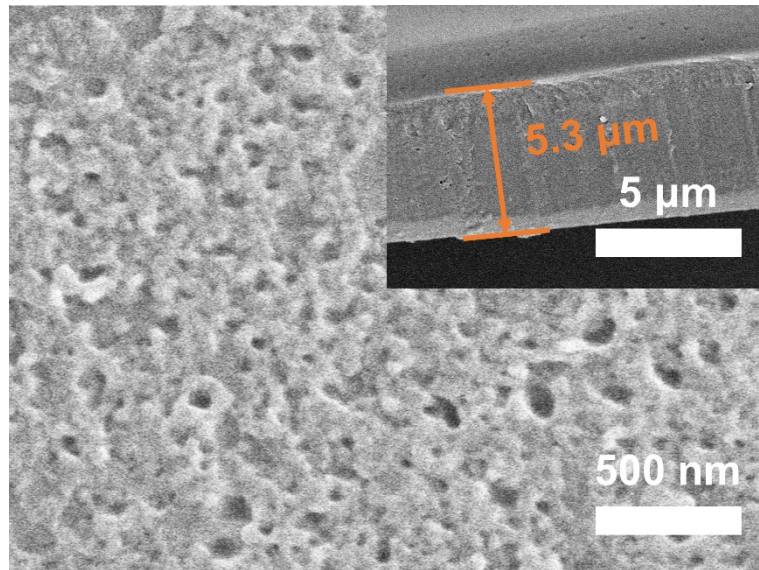


**Figure S7.** Top-view SEM image of POXIE-QA membrane. Inserted are the cross-section of the SEM image and the thickness of the membrane.

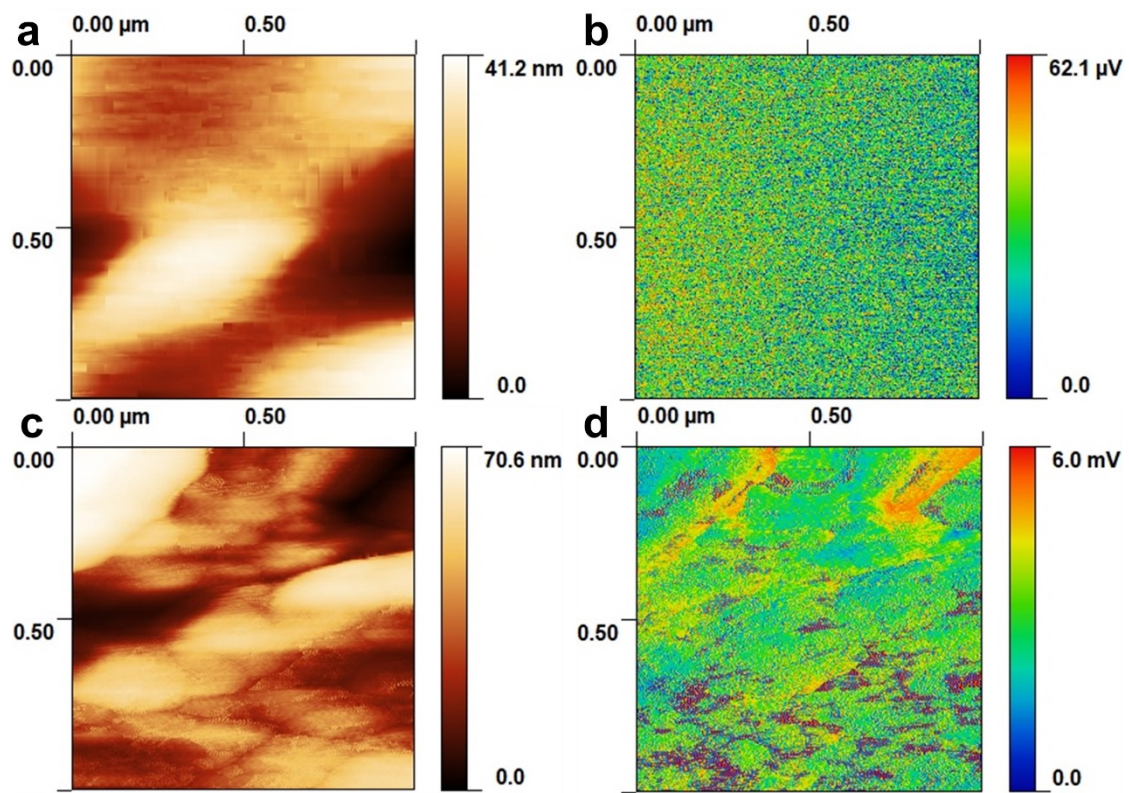


**Figure S8.** AFM topographical height image and phase image of POXIE-QA (a, b), POXIB-QA (c, d).

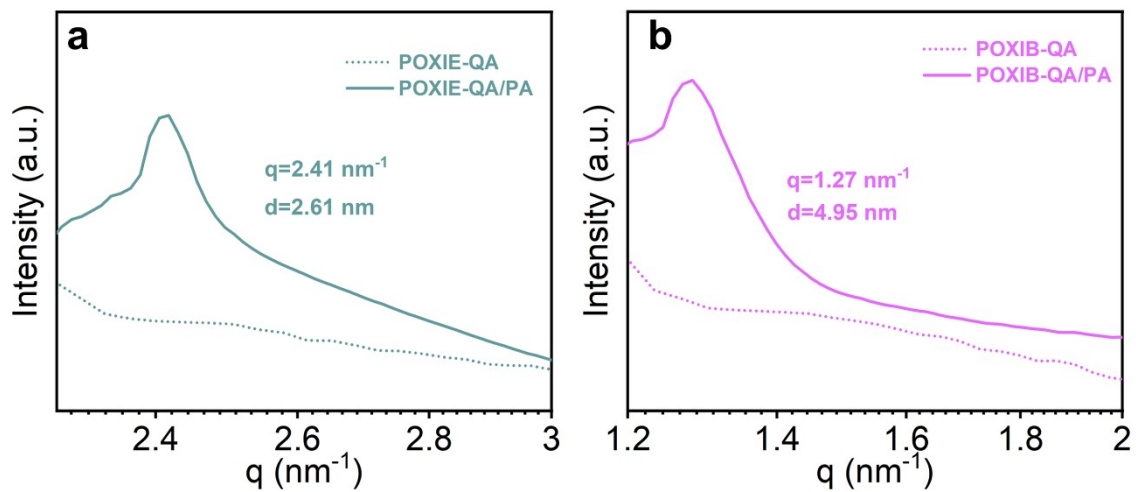


**Figure S9.** SAXS plots of (a) POXIE-QA/PA and POXIE-QA, and (b) POXIB-QA/PA and POXIB-QA.

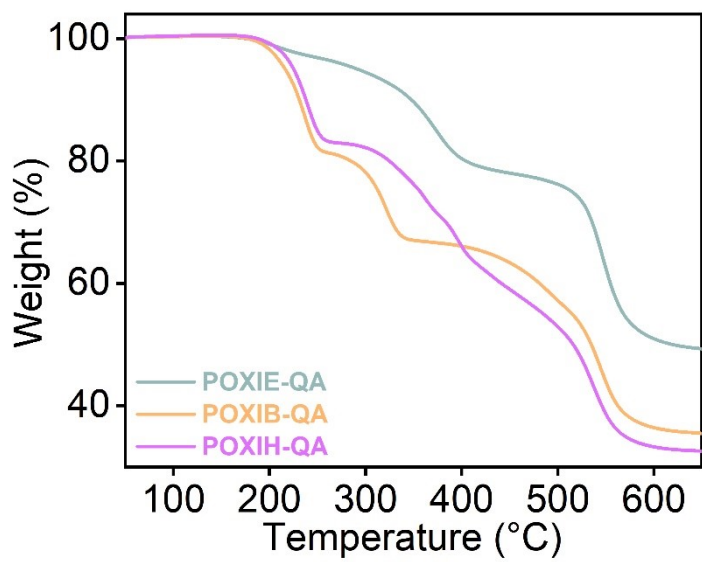


**Figure S10.** TGA curves of POXIA-QA under  $\text{N}_2$  flow (heating rate:  $10\text{ }^{\circ}\text{C min}^{-1}$ ).

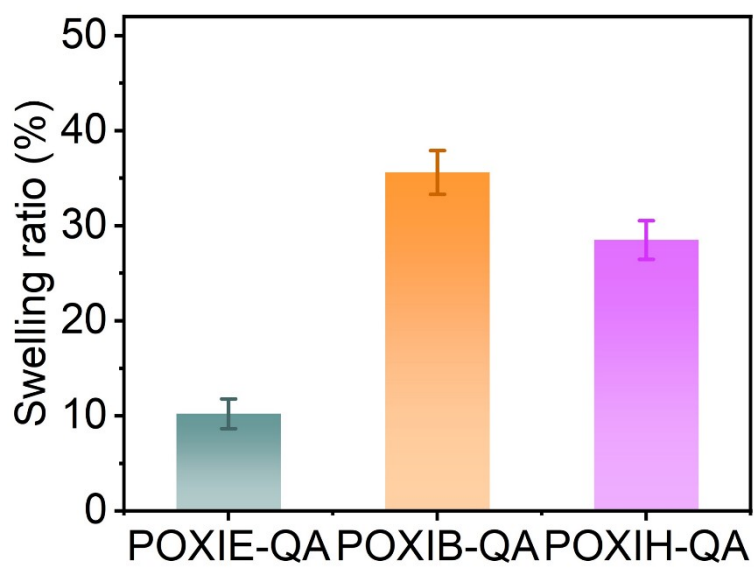


**Figure S11.** Length swelling ratios of the POXIA-QA membranes under saturated PA doping level.

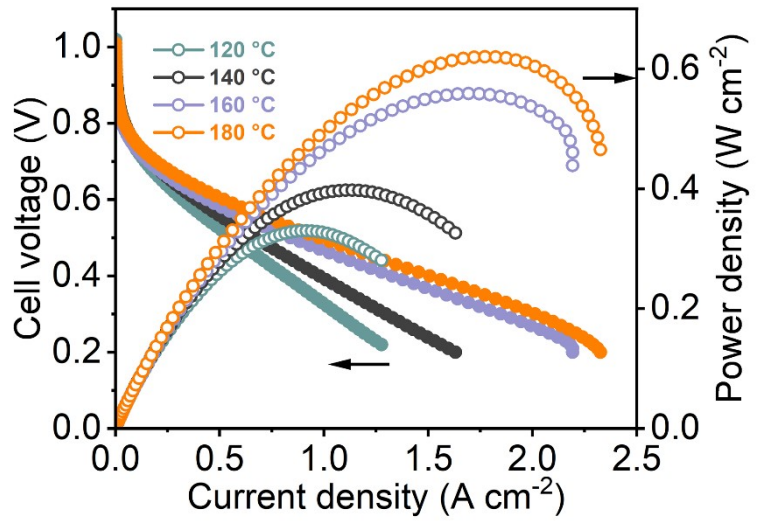


**Figure S12.** Polarization curves and power density curves of the POXB-QA/PA membrane based on  $\text{H}_2/\text{O}_2$  single cell under at different temperatures.

## Supporting tables

**Table S1.** Molecular weight and polydispersity index of POXIA-QA.

Polymer	$M_n^a (\times 10^4)$	$M_w^b (\times 10^4)$	PDI <sup>c</sup>
POXIE	1.4	3.6	2.5
POXIB	1.6	4.3	2.6
POXIH	2.4	6.8	2.8

(a) Number-average molecular weight.

(b) Weight-average molecular weight.

(c) Polydispersity index, PDI= $M_w/M_n$ .

**Table S2.** IECs of POXIA-QA with different measuring method.

Membrane	Tensile				Elongation break (%)	PDL	PA retention (%)	Swelling ratio (%)
	IEC <sub>theo</sub> <sup>a</sup> (meq/g)	IEC <sub>NMR</sub> <sup>b</sup> (meq/g)	IEC <sub>titr</sub> <sup>c</sup> (meq/g)	stress-strain (MPa)				
<b>POXIE-QA</b>	2.04	--	1.68±0.04	36.45	7.58	10.55	75.98	10.20%± 1.56
<b>POXIB-QA</b>	1.93	1.90	1.86±0.05	21.83	16.72	24.18	88.25	35.60%±2.29
<b>POXIH-QA</b>	1.83	1.83	1.75±0.05	24.50	12.86	19.97	86.03	28.50%±2.03

(a) Theoretical IEC, calculated from the ratios of completely conversion.

(b) Calculated from the <sup>1</sup>H NMR (Fig. S3) by the ratio of aromatic hydrogen at 7-8 ppm (A<sub>1</sub>) and the -CH<sub>3</sub> of piperidinium at 2.92 ppm (A<sub>2</sub>). The degree of quaternization was calculated according to the following equation:

$$\text{Degree of quaternization} = \frac{4 \times A_2}{A_1} \times 100\%$$

(c) Experimental value determined by Mohr titration.

**Table S3.** Comparison of the present work and related work on PA doping and proton conductivity.

<b>Membrane</b>	<b>IEC</b>	<b>PA doping level</b>	<b>PA retention</b>	<b>swelling ratio (%)</b>	<b>Proton conductivity at 160 °C (S cm<sup>-1</sup>)</b>	<b>Max proton conductivity (S cm<sup>-1</sup>)</b>	<b>Ea (kJ mol<sup>-1</sup>)</b>	<b>Reference</b>
POXIE-QA	1.68±0.04	10.55	75.98% (80°C/40%RH)	10.20%±1.56	0.05	0.062@180 °C	19.43	This work
POXIB-QA	1.86±0.05	24.18	88.25% (80°C/40%RH)	35.60%±2.29	0.086	0.098@180 °C	11.51	This work
POXIH-QA	1.75±0.05	19.97	86.03% (80°C/40%RH)	28.50%±2.03	0.103	0.113@180 °C	7.35	This work
IMOPBI (IM-81)	1.19 mmol/g	361.2 ± 22.9 wt.%	--	209.5 ± 13.7	0.1	0.104@170 °C	--	<sup>1</sup>
PBI-Sc-35	--	10	75%	--	0.1	0.104@170 °C	11.7	<sup>2</sup>
PBI/sGO-2	--	15	75%	--	0.118	0.136@180 °C	12.36	<sup>3</sup>
PBI/1Mus	--	13.65	--	70.99 ± 3.3	0.045	0.047@170 °C	--	<sup>4</sup>
AmPBI-Car-10		10.5	40% (80°C/40%RH)	156.7(volume swelling)	0.11	0.125@180 °C	12	<sup>5</sup>
PPBI/Mim7+/PA M2	--	15.2	90% (140°C H <sub>2</sub> O vapor)	--	0.215	0.22@180°C	7.66	<sup>6</sup>
L-10	--	18.7	65.4% (80°C/40%RH)	91% (area swelling)	0.257	0.313@200°C	--	<sup>7</sup>
QSILMs	--	5.1	--	--	0.04	0.06@180 °C	--	<sup>8</sup>
1%-PBI	--	288%	76.7% (80°C/40%RH)	--	0.168	0.17@180°C	--	<sup>9</sup>
mPBI-TzPEN25	--	323±10 %	35% (60°C/80-90%RH)	--	0.195	0.195@160°C	17.9	<sup>10</sup>
XTPPO-40-15	--	7.5±0.3	60% (80°C/50%RH)	18±1% (length swelling)	0.05	0.064@180 °C	--	<sup>11</sup>
ABPBI/5IL@SN R	--	<4	<70% (boiled water)	18.22 ± 1.2 (area)	0.04	0.04@180 °C	--	<sup>12</sup>

				swelling)				
50PPF/PBI	--	160%	<40%	60% (volume swelling)	0.06	0.062@140 °C	--	<sup>13</sup>
10%PAF-6- PA/OPBI	--	317.6%	39.82%	117.2%	0.073	0.089@200 °C	14.47	<sup>14</sup>
PA/PIBI-Q80	2.22	12.5	--	354.9% (volume swelling)	0.06	0.07@180 °C	12.3	<sup>15</sup>
PenTrip(CH <sub>3</sub> )- PyPBI	--	32	65.5%	225% (volume swelling)	0.22	0.24@180 °C	--	<sup>16</sup>
Ph(CF <sub>3</sub> )-PyOPBI	--	22.1	72%	35%	0.07	0.078@180 °C	15.38	<sup>17</sup>

**Table S4.** Comparison of the present work and related work on HT-PEMFCs.

Membrane	Fuel gas	Temperature (°C)	Pt loading (mg cm <sup>-2</sup> ) (cathode)	Max power density (W cm <sup>-2</sup> )	Reference
POXIE-QA	H <sub>2</sub> , O <sub>2</sub>	180	1.1	1.0	This work
POXIE-QA	H <sub>2</sub> , O <sub>2</sub>	160	1.1	0.86	Thi work
IMOPBI	H <sub>2</sub> , Air	160	1	0.429	<sup>1</sup>
PBI-Sc-5	H <sub>2</sub> , Air	160	1.5	0.411	<sup>2</sup>
PBI/sGO-2	H <sub>2</sub> , Air	160	1	0.364	<sup>3</sup>
PBI/1Mus	H <sub>2</sub> , Air	150	1	0.586	<sup>4</sup>
AmPBI-Car-5	H <sub>2</sub> , Air	160	1.5	0.216	<sup>5</sup>
PPBI/Mim <sub>7</sub> <sup>+</sup> /PAM2	H <sub>2</sub> , O <sub>2</sub>	180	0.5	0.610	<sup>6</sup>
L-10	H <sub>2</sub> , Air	160	0.6	0.438	<sup>7</sup>
QSILMs	H <sub>2</sub> , Air	200	1.3	0.320	<sup>8</sup>
1%-PBI	H <sub>2</sub> , O <sub>2</sub>	160	0.6	0.597	<sup>9</sup>
mPBI-TzPEN25	H <sub>2</sub> , Air	160	1	0.447	<sup>10</sup>
ABPBI/5IL@SNR	H <sub>2</sub> , O <sub>2</sub>	180	0.4	0.28	<sup>12</sup>
50PPF/PBI	H <sub>2</sub> , O <sub>2</sub>	160	1	0.607	<sup>13</sup>
PSf-TEA-110	H <sub>2</sub> , O <sub>2</sub>	160	0.65	<0.45	<sup>18</sup>

## Reference

- 1 J. Wang, G. Liu, A. Wang, W. Ji, L. Zhang, T. Zhang, J. Li, H. Pan, H. Tang and H. Zhang, *J. Membr. Sci.*, 2023, **669**, 121332.
- 2 H. Chen, S. Wang, F. Liu, D. Wang, J. Li, T. Mao, G. Liu, X. Wang, J. Xu and Z. Wang, *J. Membr. Sci.*, 2020, **596**, 117722.
- 3 Y. Devrim and G. N. Bulanik Durmuş, *Int. J. Hydrogen Energy*, 2022, **47**, 9004–9017.
- 4 Z. Guo, J. Chen, J. J. Byun, M. Perez–Page, Z. Ji, Z. Zhao and S. M. Holmes, *J. Membr. Sci.*, 2022, **641**, 119868.
- 5 Y. Cui, S. Wang, D. Wang, G. Liu, F. Liu, D. Liang, X. Wang, Z. Yong and Z. Wang, *J. Membr. Sci.*, 2021, **637**, 119610.
- 6 Z. Rajabi, M. Javanbakht, K. Hooshyari, M. Adibi and A. Badiei, *Int. J. Hydrogen Energy*, 2021, **46**, 33241–33259.
- 7 P. Wang, X. Li, Z. Liu, J. Peng, C. Shi, T. Li, J. Yang, C. Shan, W. Hu and B. Liu, *J. Membr. Sci.*, 2022, **659**, 120790.
- 8 G. Skorikova, D. Rauber, D. Aili, S. Martin, Q. Li, D. Henkensmeier and R. Hempelmann, *J. Membr. Sci.*, 2020, **608**, 118188.
- 9 J. Peng, X. Fu, J. Luo, Y. Liu, L. Wang and X. Peng, *J. Membr. Sci.*, 2022, **643**, 120037.
- 10 N. N. Krishnan, N. M. H. Duong, A. Konovalova, J. H. Jang, H. S. Park, H. J. Kim, A. Roznowska, A. Michalak and D. Henkensmeier, *J. Membr. Sci.*, 2020, **614**, 118494.
- 11 J. Jang, D.-H. Kim, M.-K. Ahn, C.-M. Min, S.-B. Lee, J. Byun, C. Pak and J.-S. Lee, *J. Membr. Sci.*, 2020, **595**, 117508.
- 12 X. Zhang, X. Fu, S. Yang, Y. Zhang, R. Zhang, S. Hu, X. Bao, F. Zhao, X. Li and Q. Liu, *J. Mater. Chem. A*, 2019, **7**, 15288–15301.
- 13 X. Hao, Z. Li, M. Xiao, D. Han, S. Huang, G. Xi, S. Wang and Y. Meng, *J. Mater. Chem. A*, 2022, **10**, 10916–10925.
- 14 L. Wang, Y. Wang, Z. Li, T. Li, R. Zhang, J. Li, B. Liu, Z. Lv, W. Cai, S. Sun, W. Hu, Y. Lu and G. Zhu, *Adv. Mater.*, 2023, **35**, 2303535.
- 15 Q. Ju, H. Tang, G. Chao, T. Guo, K. Geng and N. Li, *J. Mater. Chem. A*, 2022, **10**, 25295–25306.
- 16 Harilal, R. Bhattacharyya, A. Shukla, P. C. Ghosh and T. Jana, *J. Mater. Chem. A*, 2022, **10**, 11074–11091.
- 17 Harilal, A. Shukla, P. C. Ghosh and T. Jana, *ACS Appl. Energy Mater.*, 2021, **4**, 1644–1656.
- 18 H. Tang, K. Geng, J. Hao, X. Zhang, Z. Shao and N. Li, *J. Power Sources*, 2020, **475**, 228521.